A Model of Voltage Gating Developed Using the KvAP Channel Crystal Structure

Indira H. Shrivastava, Stewart R. Durell, and H. Robert Guy
Laboratory of Experimental and Computational Biology, Center for Cancer Research, National Cancer Institute,
National Institutes of Health, Bethesda, Maryland

ABSTRACT   Having inspected the crystal structure of the complete KvAP channel protein, we suspect that the voltage-sensing domain is too distorted to provide reliable information about its native tertiary structure or its interactions with the central pore-forming domain. On the other hand, a second crystal structure of the isolated voltage-sensing domain may well correspond to a native open conformation. We also observe that the paddle model of gating developed from these two structures is inconsistent with many experimental results, and suspect it to be energetically unrealistic. Here we show that the isolated voltage-sensing domain crystal structure can be docked onto the pore domain portion of the full-length KvAP crystal structure in an energetically favorable way to create a model of the open conformation. Using this as a starting point, we have developed rather conventional models of resting and transition conformations based on the helical screw mechanism for the transition from the open to the resting conformation. Our models are consistent with both theoretical considerations and experimental results.

INTRODUCTION

Before the crystallization of the KvAP channel structures (Jiang et al., 2003a) there was a general consensus about several aspects of the voltage-sensing mechanism of K^+ channels, based primarily on mutagenesis experiments performed on the *Shaker* K^+ channel (Durell et al., 1998; Gandhi and Isacoff, 2002; Bezanilla, 2002). In these models, the voltage-sensing domain consisted of four α-helices (S1–S4) that spanned the membrane in all conformations. Accessibility studies suggested that the positively charged residues of S4 resided primarily in water-filled crevasses, and the voltage dependency was due to the movement of these charges past a relatively short barrier. The principal dispute involved the magnitude of the movement of S4 during activation: in one class of models, the S4 helix moved past a relatively fixed central barrier, whereas in another class, the translational movement of S4 was small but the location of the barrier shifted relative to S4 (see Fig. 1).

The crystal structure of the full-length KvAP channel (Jiang et al., 2003a) (denoted as Structure 1 here) did not support either of these models. Its pore-forming domain (S5-P-S6) appears to be in an open conformation, since it closely resembles the MthK structure (Jiang et al., 2002) in which the gate formed by the inner portions of the M2 segments (which are analogous to the S6 segments of Kv channels) is open. While the secondary structure of its voltage-sensing domain is similar to those of previously developed models (e.g., Durell et al., 1998), its S1–S4 helices do not span the transmembrane region as anticipated; rather, they are

approximately parallel to the plane of the membrane. S1 and S2 helices encircled the central S5-P-S6 domain with their termini near the center of the transmembrane region, the S3b helix (the second half of segment S3) is at the cytoplasmic membrane interface, and S4 is completely in the cytoplasmic region (see Fig. 2 *A*). (These evaluations are based on positioning the pore-forming domain in the transmembrane region.) These findings suggest that either 1), previous models, and the criteria used to develop them, are flawed and the crystal structure is correct; 2), the crystal structure is grossly distorted from the native structure; or 3), KvAP has a very different structure from *Shaker*. However, striking similarities of both the voltage-dependent gating and sequence of KvAP (Ruta et al., 2003) to those of *Shaker* channels argue against the last possibility.

In an attempt to understand the complete structure of the protein and how it gates, Jiang et al. (2003b) combined Structure 1 with a second crystal structure of an isolated voltage-sensing domain (denoted as Structure 2 here) to create models of the KvAP protein (without including S1) in both open and closed conformations (see representation in Fig. 3 *A*). They proposed that although the voltage-sensing domain of Structure 1 is distorted, "the full-length channel crystal structure is actually not very far from a membrane-bound conformation" (Jiang et al., 2003a). They speculated that apparent discrepancies between their KvAP model and data from *Shaker* channels (e.g., in *Shaker* the S1-S2 loop is glycosylated and thus extracellular (Santacruz-Toloza et al., 1994) and the N-terminus of S4 is near the C-terminus of S5 when the channel is activated (Elinder et al., 2001a,b)) may be due to the highly dynamic nature of the voltage-sensing domain. The essential feature of their model is the proposal that a positively charged helical hairpin, or "paddle", formed by the C-terminus half of S3 (S3b) and S4 in both crystal structures, remains intact and moves through the lipid
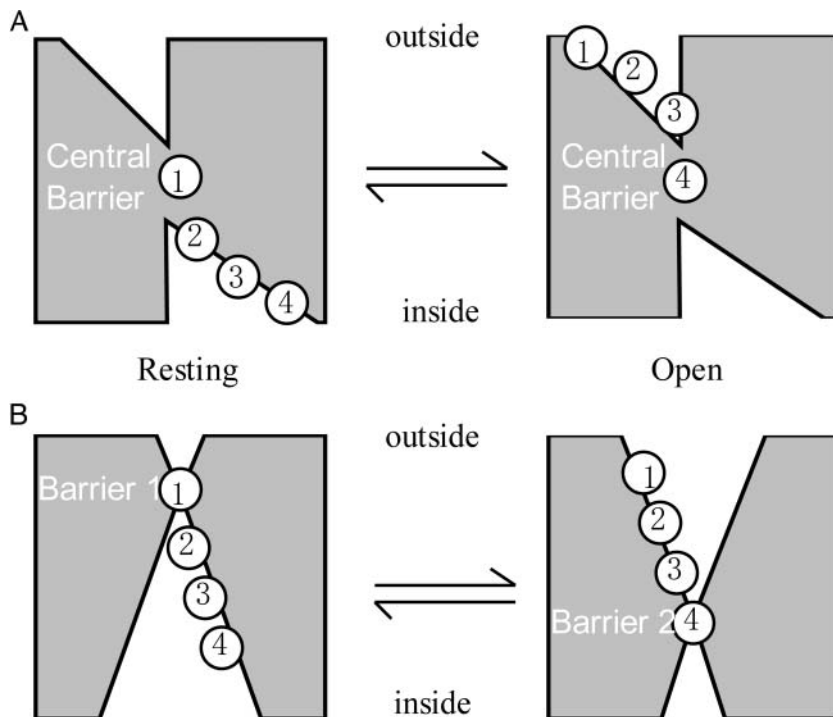
FIGURE 1 Models of voltage-sensing mechanisms involving water-filled crevasses. The numbered circles represent positively charged S4 residues. (*A*) Model in which positive charges of S4 move past a central barrier. (*B*) ''Transporter'' type model of Starace and Bezanilla (2004), in which the location of the barrier shifts but S4 does not move much.

phase of the bilayer during gating. They tested this model with experiments in which biotin molecules are attached to cysteines introduced throughout S3b and S4 (Jiang et al., 2003b). The biotin adducts bind almost irreversibly to avidin, a protein that is too large to diffuse into transmembrane crevasses. They found that biotin adducts at two positions on S4 (L121C and L122C) bind to intracellular avidin at negative voltages and to extracellular avidin at positive voltages, suggesting that these residues move ~20 Å across the transmembrane region during activation. Furthermore, they found that the accessibility to avidin of adducts attached to any residue preceding 123 in S3b or S4 is increased dramatically by depolarizing the membrane. These results were interpreted as evidence that the paddle moves

through the lipid phase during activation in a manner inconsistent with previously developed models.

The paddle model was controversial when introduced because it was inconsistent with numerous experimental results and with basic physiochemical principles commonly used in developing models of membrane proteins (Miller, 2003; Gandhi et al., 2003). Furthermore, it has not been supported by numerous recent experiments designed to test it. The theoretical inconsistencies are described later in this article, and most of the experimental inconsistencies are discussed in an accompanying article on models of the *Shaker* channel. Much of the controversy involves the extent to which the full-length KvAP crystal structure (Jiang et al., 2003a) is distorted from a native conformation. The
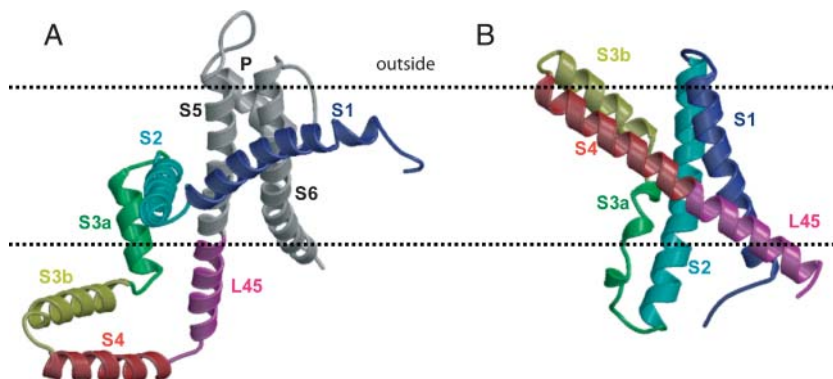
FIGURE 2 Ribbon representation of the KvAP crystal structures (Jiang et al., 2003a). (*A*) One subunit of Structure 1 of both the voltage-sensing and pore-forming domains. (*B*) KvAP crystal Structure 2 of the voltage-sensing domain in the orientation we advocate for the open conformation. The color code for the segments is S1, blue; S2, cyan; S3a, green; S3b, yellow-orange; S4, red; L45, magenta; and S5-P-S6, white. The dashed lines are 25 Å apart and designate boundaries of the hydrophobic alkyl phase of the bilayer.

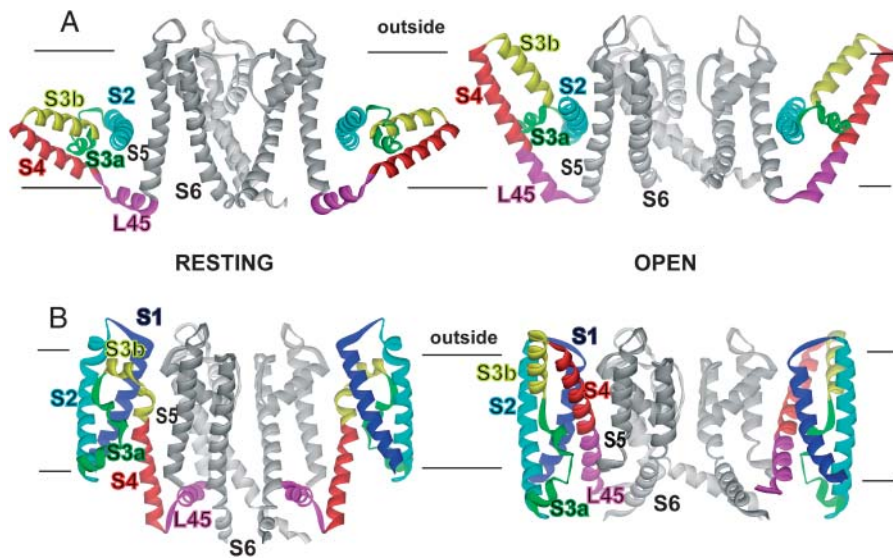FIGURE 3 Comparison of the paddle and helical screw models. Segments are colored as in Fig. 2. (*A*) Ribbon representation similar to the ''paddle'' of Jiang et al. (2003b) for gating of the KvAP gating resting and open conformations. The paddle formed by S3b and S4 remains intact as it passes through the alkyl phase of the membrane during activation. (*B*) The model presented in this study. The S1, S2, and S3a structure spans the membrane, has little contact with the pore-forming domain, and remains relatively static during gating. In the resting conformation, the L45 helix is in the cytoplasm, the S3b-S4 helix spans the bilayer and is positioned between the pore-forming domain and the S1–S3 segments. When the channel activates, S4 and L45 move toward the extracellular surface to form a single transmembrane helix and S3b jackknifes to become antiparallel to S4 on the extracellular surface. In the open conformation, the pore-forming domain structure is similar to that of KvAP crystal Structure 1 and voltage-sensing domain structure is similar to that of KvAP crystal Structure 2.

following evidence supports the interpretation that the voltage-sensing domain of Structure 1 is very distorted:

1. In native KvAP channels, Fab fragments that bind to the S3-S4 loop (located in the cytoplasm in Structure 1) do so only from the extracellular side (Jiang et al., 2003a).
2. In *Shaker* channels, residues in the latter portion of S1 and S3, in the initial part of S2 and S4, and in the S1-S2 and S3-S4 loops are accessible from the extracellular solution in all conformations (Gandhi et al., 2003) (analogous KvAP residues in Structure 1 are located on or near the opposite side of the membrane).
3. Residues immediately preceding S1 in *Shaker* channels are located in the cytoplasm (Patton et al., 1993) (in Structure 1 analogous KvAP residues are in the center of the transmembrane region).
4. Except for the S3-S4 hairpin, the tertiary structure of the voltage-sensing domain in Structure 1 deviates substantially from the crystal structure (see Fig. 2 *B*) of the isolated KvAP voltage-sensing domain, Structure 2 (Jiang et al., 2003a).

    The apparent distortion of the protein may be due to multiple factors: extraction of the protein from the lipid bilayer, the highly dynamic nature of the protein, and/or the binding of the Fab fragments.

Is there a better way to reconcile the KvAP crystal structure data with results of mutagenesis analyses of other Kv channels and basic physiochemical principals of membrane protein structure? Here we present a more conventional model of the voltage-sensing mechanism of KvAP. As with the paddle model, the open conformation of our model was developed by combining the pore-forming domain of Structure 1 with the voltage-sensing domain of Structure 2; however, the domains were docked together on the basis of experimental results and physiochemical principles. Our model has the ''traditional'' transmembrane topology, in which each of the S1–S6 segments transverses the entire transmembrane region, and much of the movement of S4 occurs via the helical screw mechanism, which is one of the oldest proposals for the motion of S4 (Guy and Seetharamulu, 1986). We consider our model to be more energetically favorable than the paddle model, because charge groups are never exposed to the hydrophobic core of the membrane. Instead, when positively charged S4 groups are in the central transmembrane region they are always near a negatively charged residue on S1, S2, or S3 (see Fig. 4 and supplementary movies), which also explains the retention of formal charge as they move from the intracellular to the extracellular membrane surface during activation. In the accompanying article on the *Shaker* channel, we explain how our models account for many experimental results which are inconsistent with, or unexplained by, the paddle model.

METHODS

The criteria we use in developing models of membrane protein are listed in the Appendix.

Most Kv channel sequences were obtained from the National Center for Biotechnology Information's nonredundant database using PsiBlast (Altschul et al., 1997), but some prokaryotic sequences were obtained from the database of unpublished microbial sequences (http://www/ncbi/nlm/nih/gov/BLAST/). Sequences were aligned using ClustalW (Thompson et al.,
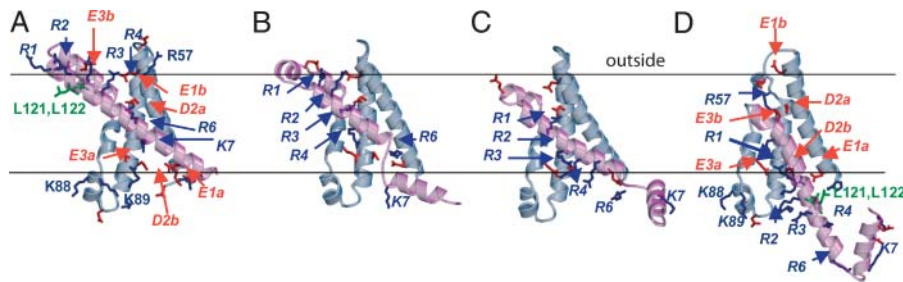
FIGURE 4 Ribbon representation of the voltage-sensing domain viewed from the side. The dashed lines are 25 Å apart and indicate the position of proposed apolar lipid interfaces. (*A*) For the open conformation, the structure is that of crystal Structure 2. (*B* and *C*) Transition conformations in which S4 has moved inwardly by two (*B*, transition 2 snapshot) or four (*C*, transition 4 snapshot) helical screw steps. (*D*) Innermost resting conformation. S1–S3a segments are gray; S3b, S4, and L45 are magenta. The S1, S2, and S3 segments do not move substantially during gating. S3b is part of the S4 helix in the resting conformation. Positively charged Arg, Lys, and His side chains are blue, negatively charged Glu and Asp side chains are red, and L121 and L122 are green. All charged residue side chains of the domain are shown in *A* and *D*; only positively charged S4 residues and the negatively charged residues in S1–S3 with which they interact are shown in *B* and *C*. See text for nomenclature of labeled residues.

1994) followed by some manual adjustments using the Seqlab editor of the GCG program (Wisconsin Package Version 10.2, Accelrys, San Diego, CA) to reduce insertions and deletions (indels) in transmembrane segments.

Profiles of the multiple sequence alignments were developed using position-based sequence weights according to the protocol of (Henikoff and Henikoff, 1994). The profiles are simply matrices listing the frequency of each of the 20 possible residue types at each linear sequence position of the alignment. The degree of mutability, or residue-type variability, used to color-code Figs. 7 and 8 was calculated from the profiles according to Eq. 1 (see Figs. 7 and 8):

$$\mu_p = (N_p - 1) \sum_{i,j=1}^{20} f_{ip} f_{jp} D_{ij}. \tag{1}$$

N_p is the total number of residue types at position p (with diminished contributions for infrequent residue types), f_{ip} is the frequency of residue type i at position p (obtained from the alignment profile), and D_{ij} is the physiochemical difference, or distance, between residue types i and j. To diminish the contribution of infrequently occurring residues (defined as a frequency <0.1), N_p was calculated according to Eq. 2:

$$N_p = \sum_{k=1}^{20} n_{kp}$$

where

$$\begin{aligned} n_{kp} &= 0, & \text{if} \quad f_{kp} = 0.0. \\ n_{kp} &= 10 * f_{kp}, & \text{if} \quad 0.0 < f_{kp} < 0.1 \\ n_{kp} &= 1, & \text{if} \quad f_{kp} \geq 0.1 \end{aligned} \tag{2}$$

The distance matrix values D_{ij} were calculated according to Eq. 3 from the S_{ij} elements of the Persson-Argos 80 similarity matrix (Ng et al., 2000), which was developed from an analysis of transmembrane segments:

$$D_{ij} = \frac{S_{ii} S_{jj}}{2.0} - S_{ij}. \tag{3}$$

Equation 1 was developed to provide a position-specific mutability parameter with the following properties: 1), equals zero when only one residue type is present at a specific position; 2), increases as the number of residue types increase; 3), is not substantially affected by rare sequencing errors or nonfunctional mutant sequences in the database (corrected for by Eq. 2 when $f_{ij} < 0.1$); 4), is not unduly influenced by a disproportional number of highly similar sequences in the alignment (by using the above-cited sequence-weighting algorithm in constructing the profiles); and 5),

increases as the specific residue types become less physiochemically similar (which results from the $\Sigma f_{ip} f_{jp} D_{ij}$ term).

Initial structural models of the open conformation were developed using the PSSHOW program (Swanson, 1995) to manually position the structural elements taken from the 1ORQ (Structure 1) and 1ORS (Structure 2) KvAP crystal structures (Jiang et al., 2003a) and to model linkers. The rationale for the docking of the domains is described in the text. Modeling the voltage-sensing domain of transition and resting conformations required repositioning the S4 and L45 segments. For most transition conformations between open and resting conformations, S4 was positioned by matching backbone residues N of one copy of S4 to residues $(N + 3x)$, where $x = 1, 2, 3,$ or 4 indicates the number of helical screw steps that S4 was moved inwardly from Structure 2 as described in the text. Some adjustments were made manually to reduce steric clashes and to improve energetically favorable interactions such as salt bridges. When side-chain conformations were changed, rotamer angles were selected that are observed frequently in known structures for that residue type. The initial position of the L45 helix was adjusted manually so that the number of nonhelical residues linking S4 to L45 and L45 to S5 remained relatively small, and so that the hydrophilic and hydrophobic faces of L45 remained in hydrophobic and hydrophilic environments. The subunits were constrained to have fourfold symmetry when the voltage-sensing domain was docked onto the pore-forming domain. Structure 1 was used to model the structure of the open pore-forming domain. The closed conformation was modeled by adjusting the positions of the S5 and S6 segments to correspond to the backbone structure of the KcsA crystal (Zhou et al., 2001). Nonhelical segments that connected the two domains or that changed conformations for the models of the transition and resting conformations were initially modeled manually. These structures were then minimized using CHARMM (Brooks, 1983). This process was repeated with adjustments if the structure of S1–S3 or secondary structure of S4 was perturbed substantially, or if side chains adopted energetically unfavorable conformations during the minimization. The models were analyzed with ProCheck (Laskowski et al, 1993) to ensure that the properties of the structures were realistic (see Table 1 of supplementary material).

The molecular dynamics simulations were run using the program Gromacs (http://www.gromacs.org). Coordinates for the phosphatidyletha-nolamine (POPE) lipid bilayer were kindly provided by Dr. Peter Tieleman. The electrostatic calculations were done using the particle mesh Ewald method, and the Van-der-Waals cutoff was 1.0 nm. The time step was 2 fs and the LINCS algorithm was used to constrain bond lengths. The simulations were run under NPT conditions (Number of atoms, Pressure, and Temperature were kept constant) with the protein, lipid and water each coupled separately to a temperature bath at 310 K with a coupling constant τ_T of 0.1 ps, and at a constant pressure of 1 bar in all directions with a pressure constant of $\tau_p = 1.0$ ps. The lipid parameters were based on Berger et al (1997), and the lipid-protein interactions were based on the GROMOS parameters. Potassium ions were placed at the putative binding

sites in the selectivity filter and the cavity, as in the KcsA crystal structure (Zhou et al., 2001). Each simulation was preceded by an energy minimization using the steepest descent method. This was followed by a short equilibration run of 200 ps with harmonic restraints on the backbone atoms of the protein to allow packing of the lipid molecules around the protein and relaxing of the water molecules. Each simulation was run for 1 or 2 ns on a dual athlon processor, which took ~10 days or less, depending on the size of the simulation system, which varied from ~45,000 atoms (isolated voltage sensor domain simulation models) to ~80,000 atoms (four pore-forming domains + voltage sensor domain of one subunit). In models in which residues of voltage-sensing domains from adjacent subunits did not interact with each other, only one voltage-sensing domain was included in the simulation to reduce the computational time. The nonbonded interaction-energy calculations were based on the contributions of the Coulombic short-range, Lennard-Jones short-range and long range potential interaction energies, averaged over the last half of the simulation periods.

RESULTS

Orientation of the voltage-sensing domain in the membrane

In developing our models, we first treat the pore-forming and voltage-sensing domains as if they were independent entities to approximate their position and orientation in the lipid bilayer and to assess the stability of each isolated domain. Our assumption that each domain should be relatively stable in a lipid bilayer when isolated from the other is based on the following observations:

1. Numerous 2TM K^+ channel families do not possess a voltage-sensing domain and at least one protein (Kumanovics et al., 2002) has a voltage sensing domain but no pore-forming domain.
2. The crystal structures of the pore-forming domain of three distantly related 2TM K^+ channels (KcsA (Doyle et al., 1998), MthK (Jiang et al., 2002), and KirBac1.1 (Kuo et al., 2003)) are quite similar to that of the KvAP pore-forming domain of Structure 1.
3. A chimera in which a *Shaker* channel pore-forming domain is replaced with that of KcsA functions (Lu et al., 2001), indicating that the protein functions even when most specific residue-residue interactions between the two domains are probably altered.
4. The transmembrane surface of the KvAP pore-forming domain that could interact with that of the voltage-sensing domain has few polar atoms and few of these surface residues are highly conserved; thus, almost all interactions between the two domains in the trans-membrane region will be hydrophobic and should be mimicked reasonably well by lipid alkyl chains.
5. Molecular dynamics simulations, described below, indicated that each domain is quite stable when embedded in a lipid bilayer.

In predicting how transmembrane portions of membrane crystal structures are likely to be positioned in the lipid bilayer, we first visually examine the structures to identify two parallel transition planes between hydrophobic surface residues that are likely to be exposed to lipid alkyl chains, and hydrophilic surface atoms that are likely to be exposed to water and/or lipid headgroups. These planes are 25 Å apart (White and Wimley, 1998). For Structure 2 of KvAP we identified an outer transition plane bordered on the polar side by the C-terminus of S1, and guanidium groups of R57 (the fourth residue of S2) and R117 (*R1*), R120 (*R2*), and R123 (*R3*) of S4 (italics indicate use of a generic nomenclature for some charged residues of the voltage-sensing domain); and an inner transition plane bordered by the N-terminus of S1, C-terminus of S2, and amine groups of the K88 and K89 residues at the beginning of S3 (see Fig. 4 *A*).

The S4-L45 helix has too many hydrophilic residues to be predicted to be a transmembrane helix by most algorithms designed to identify hydrophobic transmembrane helices. However, for the transmembrane orientation in Fig. 4 *A*, almost all of these residues are in the hydrophilic core of the voltage-sensing domain and/or are positioned where they can interact with polar lipid headgroups and water at the membrane-water interface. The length of the KvAP S4-L45 helix (33 residues or ~50 Å) allows it to transverse the transmembrane region in this tilted orientation. The extreme tilt of the S4-L45 helix relative to the other helices and to the membrane's normal creates a hydrophilic region above S4 on the extracellular surface and below S4-L45 on the intracellular surface (see Fig. 4 *A*). Indeed, hydrophilic cavities, or crevasses, have been predicted to exist from results of accessibility studies of residues on S2, S3, and S4 of *Shaker* and Na^+ channels (Larsson et al., 1996; Yang et al., 1996). In our models of the complete protein structure described below, these hydrophilic clefts face toward the pore-forming domain, isolating them from the hydrophobic phase of the membrane. The region where the axis of S4 and S2 cross, is relatively inaccessible from either side. We denote this region as the ''central barrier.''

Conformational changes of the voltage-sensing domain during gating

Next, models were made for the voltage-sensing domain in transition and resting configurations. With Structure 2 in the orientation of Fig. 4 *A*, L121 and L122 are near the extracellular surface, consistent with this structure corresponding to the open conformation. (Biotin adducts to L121 and 122 bind to extracellular avidin at positive voltages (Jiang et al., 2003b)). Furthermore, most of the positively charged residues of S4 are on the extracellular side, as would be expected for an open conformation. Numerous experiments indicate that virtually all of the voltage dependence of activation gating in *Shaker* is due to movement of the first four positively charged residues of S4 through the electric field of the membrane (Aggarwal and MacKinnon, 1996; Schoppa et al., 1992; Gandhi and Isacoff, 2002; Bezanilla, 2002).

What is the most energetically favorable pathway for charges on S4 to cross the electric field of the membrane in a manner that allows its titratable groups to remain charged? In KvAP, S1, S2, and S3 segments each possess two negatively charged residues, which here will be called *E1a* and *E1b* (on S1), *D2a* and *D2b* (on S2), and *E3a* and *E3b* (on S3), all of which are located in the core of the voltage-sensing domain (see Fig. 4 *B*). *E1b*, *D2a*, and *E3b* should be accessible from the outside (the residue analogous to *D2a* is outwardly accessible in *Shaker* (Tiwari-Woodruff et al., 2000) and *E1b* and *E3b* are even nearer the extracellular surface) and *E1a*, *D2b*, and *E3a* should be accessible from the inside in all conformations of our models. The six positively charged S4 residues will be called *R1*, *R2*, *R3*, *R4*, *R6*, and *K7* (the number 5 is skipped because KvAP has no charged residue at this position, but many homologous channels do; see Fig. 7). In Structure 2 of Fig. 4 *A*, *R1* and *R2* are exposed to the extracelluar aqueous phase, *R3* is exposed but near *E3b*, *R4* is near *E1b*, *R6* salt-bridges to *D2a*, and *K7* is near *D2b*. If the charged S4 side chains remain in the core of the voltage-sensing domain, then interaction with the electronegative polar core should lower the electrostatic barrier greatly and allow the residues to remain protonated. In the helical screw model (Guy and Seetharamulu, 1986), the S4 helix translocates along and rotates about its axis so that the arginines remain in the same spiral pathway as they traverse the transmembrane region. One inward helical screw step places the backbone of the nth residue in the position occupied by the $(n + 3)^{\text{th}}$ residue of the previous conformation; e.g., the helix translates by ~4.5 Å along and rotates by ~60° about its axis. Initial helical screw steps from the Structure 2 conformation result in an increase in the number of electrostatic interactions between positively and negatively charged residues; e.g., after two helical screw steps the following series of salt bridges span the transmembrane region: *R1-E3b*, *R2-E1b*, *R3-D2a*, *R4-D3a*, *R6-E2b*, and *K7-E1a* (see Fig. 4 *B*). Thus, the negatively charged residues of S1, S2, and S3 are positioned in the crystal structure in a manner that complements the spiral of positively charged S4 residues. Calculations of the mutability of residues among numerous families of distantly related

voltage-gated channels support our hypothesis that this putative transition conformation occurs in many distantly related families of voltage-gated channels (see criterion 12 of the Appendix). For this analysis, we aligned sequences from two families of prokaryotic Kv channels, several families of eukaryotic K^+ channels (Kv, Kcnq, Keag, plant, and paramecium), cyclic nucleotide-gated channels, all four homologous repeats of Na^+ and Ca^{2+} channels, and polycystin channels, and calculated the mutability of residues at each position of the multisequence alignments (see Methods and KvAP sequence of Fig. 7 for color-coded mutability results). These calculations showed that residues in the core of the central barrier are highly conserved among these families in the S1–S3 segments. Several S4 residues are also conserved among these channels. While the highly-conserved S4 residues are not in the central barrier in Structure 2, they are there in the putative transition conformation in which S4 has moved inward by two helical screw steps (see Fig. 5).

These two inward helical screw steps from Structure 2 are not sufficient, however, to move S4 to a position consistent with data for the resting conformation of either KvAP or *Shaker* channels. Two more helical screw steps move S4 to a configuration in which all but the first S4 arginine should be accessible from the intracellular surface to small reagents (Fig. 4 *C*). This conformation is consistent with data for the resting conformation of the *Shaker* channel (see accompanying article). However, additional inward movement of the KvAP S4 may be required to explain the accessibility to intracellular avidin of biotin labels attached to the L121C and L122C KvAP mutants and/or to explain why biotin labels attached to positions on the initial portion of S3b become relatively inaccessible to extracellular avidin at hyperpolarized voltages (Jiang et al., 2003b). Additional translation of KvAP's S4 can place L121 and L122 very near the intracellular interface where R1 binds to D2b and E3a and the remaining positively charged S4 residues are in the cytoplasm where they interact with lipid headgroups (Fig. 4 *D*). The large translation of S4 requires that the S3b segment moves inward at negative voltages, which explains why the accessibility of biotin adducts to S3b residues is reduced at
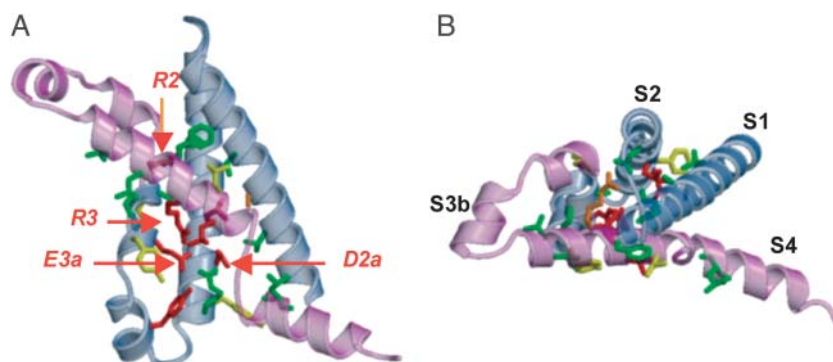
FIGURE 5 (*A*) Same transition conformation as Fig. 4 *B* except that residues are colored according to their mutability among several distantly related families of 6TM channels (see KvAP sequence in Fig. 7 *B*). Red (very highly conserved, ($\mu < 4$);orange ($4 < \mu < 8$); yellow ($8 < \mu < 12$); green (moderately conserved, $12 < \mu < 16$); white, no side chain (poorly conserved, $\mu > 16$). (*B*) View from the outside of the same structure to show that conserved residues are in the core of the domain.

negative voltages (Jiang et al. 2003b). S3 hinges at the junction between S3a and S3b in our model. Electrostatic and hydrophobic interactions of this model can be improved by altering conformation for the S1-S2 linker (see Fig. 4 *D*).

Our models were deliberately developed to maintain most of the helical secondary structure of the crystals. This was accomplished by changing backbone conformational changes at only a few hinge points: one linking S3a to S3b, one in the middle of S3b (breaking it into two helices, S3b1 and S3b2, in some transition states), one linking S3b2 to S4, one linking S4 to L45, and one linking L45 to S5. The S3b helix of the crystal structure ''jackknifes'' as S4 moves inwardly and becomes an N-terminus addition to the S4 helix in the resting conformation. The location of the putative S3b hinge was predicted to occur at E107-G108-H109 in KvAP, based on the following observations:

1. Other K^+ channels with similar length S3-S4 segments have indels and/or a proline in this location; e.g., in Fig. 7 residues 112–113 (P–S) of the KvVP sequence aligns with KvAP residues 107–109 (EGH) (see criterion 6 of the Appendix).
2. Glycine residues are frequently nonhelical.
3. Residues at the beginning and end of transmembrane helices are often hydrophilic.

The ''snapshots'' of transition locations of S4 in Fig. 4 are not intended to correspond to energy minima of kinetic schemes. Our intention to illustrate the general transition pathway is depicted more clearly in two movies made by including additional positions between each of the helical screw steps, and between the last helical screw step and final putative resting conformation (supplements to Fig. 4). The major point of the movies is to illustrate how positively charged S4 residues can move from one membrane surface to the other in an energetically favorable manner by passing though the electronegative core of the voltage-sensing domain.

Interactions between the pore-forming and voltage-sensing domains

The next step in the modeling process was to dock the two domains together and form the covalent linkage between L45 and S5. The pore-forming domain of Structure 1 was used for the open conformation. S5 and S6 segments of closed conformations of KvAP were modeled after the structure of M1 and M2 in KcsA (Zhou et al., 2001; Doyle et al., 1998), in which the inner portion of the pore formed by M2 segments is closed. Our models are tentative because there are no direct data for specific interactions between the domains in KvAP channels. Also, the hydrophobic nature of the exterior of both domains makes it difficult to identify likely interactions, or even to exclude the possibility that the transmembrane portions of the two domains have no direct

noncovalent contact in some or all conformations. We have assumed that the interactions between S4 and the pore-forming domain in KvAP are similar to those in *Shaker* (for which there are data), that interacting residues between the domains are likely to be more conserved than are residues exposed to lipids, and that the voltage-sensing domain docks on the pore-forming domain so that water-filled crevasses above and below the central barrier form in between the two domains. Ribbon representations of our models are shown in Fig. 3 *B* and Fig. 6.

We utilized information about the tolerance of residues to guide docking of the two domains. Effects on activation gating when *Shaker* or DRK1 eukaryotic Kv channel residues were replaced by either tryptophan (Hong and Miller, 2000; Monks et al., 1999) or alanine (Li-Smerin et al., 2000a,b) have been measured. Positions were considered tolerant if the mutations had little effect on gating properties. We have also made predictions of tolerance based on analyzing the variabilities (or mutabilities) of residue types at each position in multisequence alignments (Guy, 1990; Guy and Durell, 1994; Durell et al., 1998). Here we have used a new method to calculate mutabilities (see Methods) and have incorporated recently determined sequences (see Fig. 7). Residues are classified as tolerant if their mutability is high (see Fig. 7 legend). The premise of both the experimental and theoretical analyses is that residues that are on the surface in all conformations and not involved in functional processes will be tolerant; whereas those buried in the protein will be intolerant, especially if they are functionally important. These two approaches produce fairly similar results; e.g., both methods have predicted the same faces of S1 and S2 to be exposed to lipids in all conformations (see helical wheel representation of eukaryotic Kv channels in Fig. 8). The main disadvantages of the experimental approach are that it has been applied only to some segments of two members of a single eukaryotic K^+ channel family (which may not be applicable to other families) and it examines the effects of mutations to only one or two residue types at each site. The main disadvantages of the theoretical approach are that the reason why specific residues are conserved is not determined, and it is not obvious how to best calculate position-specific mutability or variability. Fortunately, we have observed that the patterns of mutability are generally quite robust and are not affected dramatically by the specific method used to calculate the mutabilities; e.g., the patterns represented in the helical wheels of Fig. 8 are quite similar to those we published earlier (Durell et al., 1998) using a simpler method and fewer sequences to calculate the mutability. We have found the theoretical approach to work best for identifying surface residues if each alignment is restricted to a distinct family of closely related proteins for which numerous sequences are known. Predictions for surface residues made by the theoretical approach have proved to be valid when applied to the KcsA and KirBac1.1 structures (Durell and Guy, 1999,
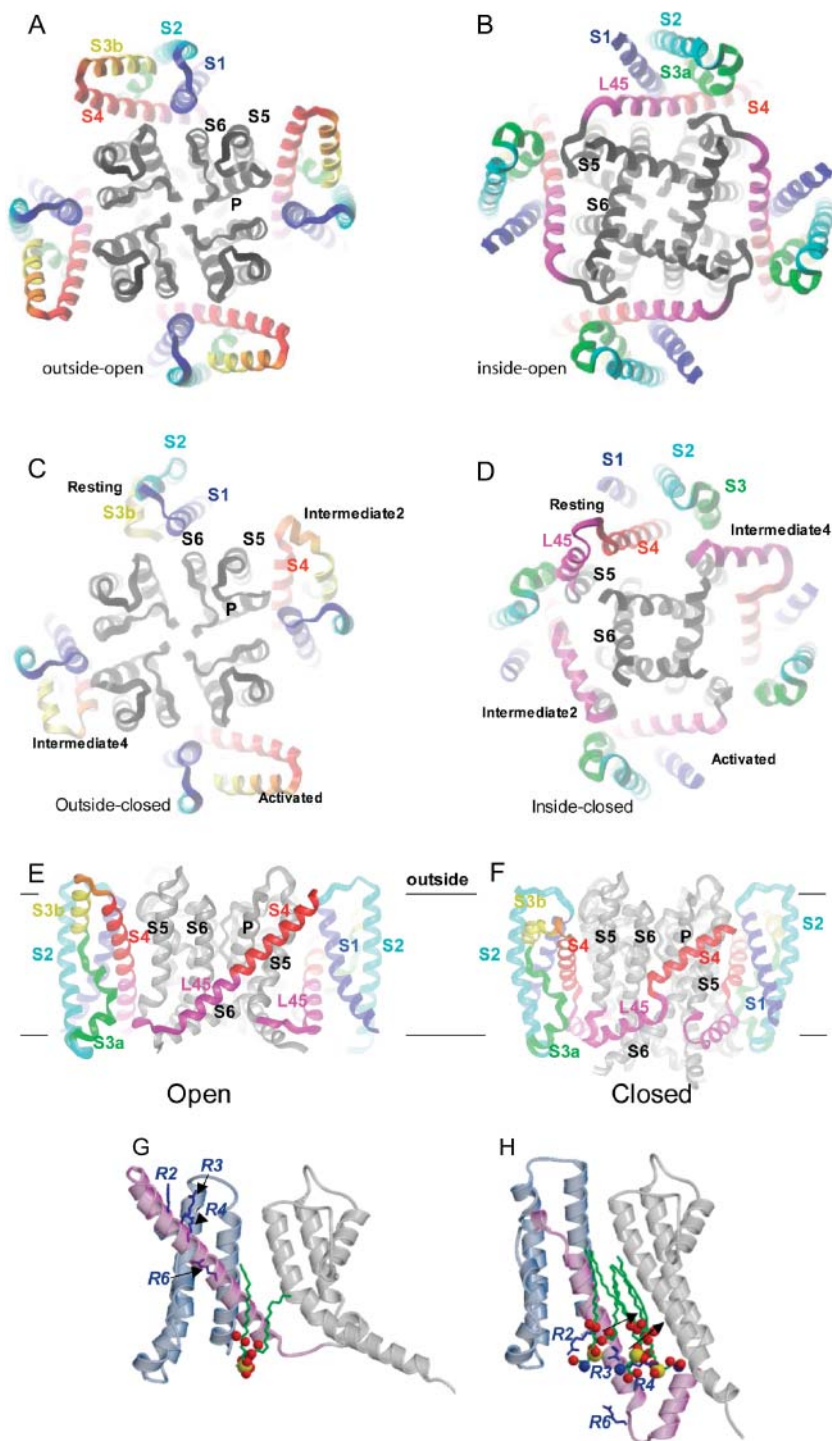
FIGURE 6 Ribbon representations of our models of the interactions between the pore-forming and voltage-sensing domains. The color scheme is the same as for Fig. 2. (*A*) Open conformation viewed from the outside. (*B*) Open conformation viewed from the inside. (*C*) Closed conformations viewed from the outside with the voltage-sensing domain in four different conformations (top is the outermost, right is transition of Fig. 4 *B*, left is transition of Fig. 4 *C*, bottom is resting conformation of Fig. 4 *D*). (*D*) Same as *C* except that the structure has been rotated by 180° about the *y* axis to show the view from the inside. (*E*) Side view of the open conformation showing S4–L45 near the viewer and portions of two voltage-sensing domains on each side of the pore-forming domains. (*F*) Side view of a closed conformation in which S4 has moved four helical screw steps inward. (*G*) Side view of one subunit in the open conformation showing the position of a lipid molecule that packs between the domains. S1, S2, and S3a are gray; S3b, S4, and L45 are magenta; and the pore-forming domain is white. Arginine side chains of S4 that interact with lipid headgroups are illustrated in blue. Lipids are colored by atom type: green, carbon; red, oxygen; blue, nitrogen; yellow, phosphorus. (*H*) Side view of one subunit in the resting conformation showing three lipid molecules that pack between the domains.

2001), the photosynthetic reaction center (Rees et al., 1989), and G protein-coupled receptors (Baldwin et al., 1997). The conclusion that the experimental results for residue tolerances are consistent with Structure 2 being a native structure has already been reported (Cohen et al., 2003). We have concentrated on results of the theoretical approach, because it provides us with information for both domains derived from both prokaryotic and eukaryotic K$^+$ channels.

Here we report results from two different multisequence alignments; one for the eukaryotic Kv family, and one for a family of bacterial Kv's that have sequences intermediate between those of the eukaryotic Kv's and that of KvAP. (Unfortunately, there are not enough close homologs to KvAP to perform this analysis for a KvAP-type family). In Fig. 7 and supplement B of Fig. 8 we have color-coded the tolerant residues into three categories: black if they are

```
Shaker: ARVVAIISVFVILLSIVIFCLETLPEFKH(19) :254
KvVP  : GRAFDIALIIAIISSLAVLVLDSIPSVRA.... : 55
KvAP  : HPLVELGVSYAALLSVIVVVVEYTMQLSG.... : 52
             1a     S1          1b
```

```
Shaker: DITDPFFLIETLCIIWFTFELTVRFLACPNKLN :306
KvVP  : EWAKELKYLEYTFTGLFTIEYLLRLYCSPKPVA : 88
KvAP  : EYLVRLYLVDLILVIILWADYAYRAYKSGDPAG : 85
             2a     S2      2b
```

```
Shaker: FCRDVMNVIDIIAIIPYFITLATVVAEEE(22) :357
KvVP  : YAKSFYGIVDLLAIIPTYLVLFFP.SASF.... :116
KvAP  : YVK..KTLYEIPALVPAGLLALIEGHLAG.... :112
         S3a 3a       S3b1    3b S3b2
```

```
Shaker: LAILRVIRLVRVFRIFKL.SRHSKGLQILGRTL :389
KvVP  : MGVIRALRVMRIFRILKL.VRYLQESNILLRSL :148
KvAP  : LGLFRLVRLLRFLRILLIISRGSKFLSAIADAA :145
         1  2S43 4  5    6 7  L45
```

```
Shaker: KASMRELGLLIFFLFIGVVLFSSAVYFAEAGSE :422
KvVP  : LMARRKIFIFFTTVAILVTIFGSLIFIVEG..P :179
KvAP  : D.KIR.FYHLFGAVMLTVLYGAFAIYIVEYPDP :176
                      S5
```

```
Shaker: NSFFKSIPDAFWWAVVTMTTVGYGDMTPVGV-- :453
KvVP  : ENGFTSIPKSIYWAIVTITTVGYGDLVPQTN-- :210
KvAP  : NSSIKSVFDALWWAVVTATTVGYGDVVPATP-- :207
                      P
```

```
Shaker: WGKIVGSLCAIAGVLTIALPVPVIVSNFNYFYH :486
KvVP  : LGKALASITMLLGYSILAVPTGIFTAELHQEMQ :243
KvAP  : IGKVIGIAVMLTGISALTLLIGTVSNMFQKILV :240
                      S6
```

FIGURE 7 Alignment of transmembrane segments from the *Shaker*, a bacterial Kv protein (KvVP), and KvAP. The *Shaker* sequence is colored according to the mutability, μ, of residues calculated from a multisequence alignment of eukaryotic Kv channel sequences; the KvVP sequence from *Vibrio parahaemolyticus* is colored according to the mutability of residues within a prokaryotic family of putative 6TM channels with sequences intermediate between those of eukaryotic Kvs and KvAP. Color code for KvAP and KvVP: red, highly conserved, $\mu < 1$; orange, $1 < \mu < 3$; yellow, $3 < \mu < 7$; green, $7 < \mu < 10$; black, $\mu > 10$ hydrophobic, likely exposed to lipid alkyl chains; dark blue, $\mu > 10$, hydrophobic and polar with high propensity for lipid headgroups; light blue, $\mu > 10$, hydrophilic, likely exposed to water. The KvAP sequence is colored according to the mutability of residues among numerous distantly related families of 6TM channels, as described in Fig. 5. Simplified numbers of charge residues in the voltage-sensing domain that interact during the helical screw transitions are colored red (negative) and blue (positive S4) below the KvAP sequence. Helical segments of the KvAP crystal structures are underlined. The parentheses indicate insertions of the indicated number of residues in the *Shaker* S1-S2 and S3-S4 loops. Our alignment differs from that of Jiang et al. (2003a) in that there is no indel in the S5 helix.

predicted to be exposed to lipid alkyl chains, dark blue if they are predicted to be in the lipid headgroup regions, and light blue or cyan if they are predicted to be exposed to the aqueous phase (see criterion 11 of the Appendix and Methods for how the mutability is calculated).

Some aspects of our models were constructed to be consistent with these predictions (see Fig. 8), whereas other

aspects were satisfied by the original crystal structures. The cores of the two domains that come directly from the crystal structures are highly conserved in both families (see *red*, *orange*, and *yellow* residues in Fig. 8), as would be expected for a native structure (criterion 12 of the Appendix). Specifically, S1 and S2 have properties that we consider indicative of transmembrane α helices, i.e., they have one poorly conserved hydrophobic face that is exposed to lipid alkyl chains, and an opposite, more highly conserved, more polar face, that interacts with other transmembrane segments. The lengths of the predicted lipid-exposed faces of S1 and S2 are just sufficient to span a 25-Å thick alkyl bilayer phase if the helices are approximately orthogonal to the plane of the membrane, as proposed above. The transition planes between predicted lipid-exposed (*black* or *dark blue*) and water-exposed (*light blue*) residues are relatively clear-cut and are located as predicted in Fig. 4, even though this orientation in the bilayer was predicted initially from Structure 2 without considering other sequences (see Fig. 8, supplement B). In Structure 2, most of the exposed surface residues on S1, S2, and S3 are tolerant (see Fig. 7). This observation suggests that most of the interactions between the two domains involve S4, which is much less tolerant. There are a few highly conserved surface residues (*red* or *orange*) near the extracellular surface in both domains of the open conformation, i.e., near the C-terminus of S1 and on S4 of the voltage-sensing domain, and near the C-terminus of S5 and N-terminus of the P-helix in the pore-forming domain. We thus docked the two domains of the open conformation together in a manner that allows interactions among these highly conserved residues. This docking arrangement has the additional advantage of being consistent with experimental studies of *Shaker* channels, which indicate that residues in the N-terminus portion of S4 interact with residues in the C-terminus of S5 of an adjacent subunit (see accompanying article). The transmembrane surface of the pore-forming domain has a groove between adjacent S5 segments into which the S4 segment can be docked in two ways to reach from the outer C-terminus of S5 of one subunit to the inner N-terminus of S5 of an adjacent subunit. Laine et al. (2003) have proposed that S4 docks in the groove with a tilt of $\sim -15°$, and interacts with the S5 segment in a clockwise manner as viewed from the outside. However, this scheme is inconsistent with our model of the voltage-sensing domain. We therefore propose that S4 docks in this groove with a tilt of $\sim 60°$, and interacts with S5 of the adjacent subunit on the counterclockwise side (see Fig. 6 *E*). This orientation is also more consistent with mutagenesis experiments on the drk1 channel, in which effects of mutating surface residues of the pore-forming domain on activation gating were measured (Li-Smerin et al., 2000a).

This docking was highly constrained by several factors:

1. The general orientation of the voltage-sensing domain relative to the membrane is limited by the positions of the
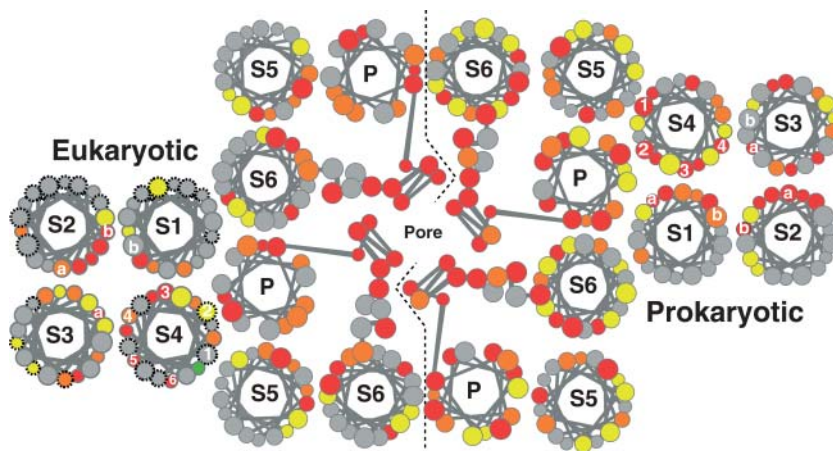
FIGURE 8 Use of mutability analyses of Kv channels in docking the voltage-sensing domain on the pore-forming core. Helical wheel representation of transmembrane segments of the pore region and one voltage-sensing domain as viewed from the outside. More highly conserved residues (*red*, *orange*, and *yellow*) are colored according to the mutability as in Fig. 7 for the prokaryotic (*right*) and eukaryotic (*left*) Kv families. Residues that have black-dashed borders indicate positions of the eukaryotic Kv family that are classed as tolerant because mutations to both tryptophan (Monks et al., 1999; Hong and Miller, 2000) and alanine (Li-Smerin et al., 2000b) in S1–S3 or to alanine in S4 (Li-Smerin et al., 2000b) had little effect on activation gating. The charged residues in S1–S4 are labeled as in Fig. 4, *B* and *C*. The wheels are convenient for illustrating that most transmembrane helices have one highly conserved face that likely interacts with other protein segments and an opposing poorly conserved face that is likely to be exposed to lipid, but do not accurately reflect the tilts of the helices or the nonhelical nature of the central portion of the S3 segment. Supplementary figures illustrate distributions of residues of differing mutabilities for a model of a closed transition conformation in which S4 has moved inwardly one helical screw step from the open conformation. Distributions of residues of differing polarities are also illustrated.

planes between surface hydrophobic and hydrophilic atoms described in the previous section.

2. The length of the S4-L45 helix is just sufficient to span the distance (~46 Å) from the C-terminus of S5 of the adjacent subunit (which interacts with the N-terminus of S4 in *Shaker*) to the N-terminus of S5 of the same subunit (to which L45 binds covalently).

3. Interactions between the C-terminus end of S1 and the pore forming domain on the extracellular surface limit the rotation of the voltage-sensing domain to the right.

4. Interactions between the N-terminus of S3 (or the S2-S3 linker) and the pore-forming domain on the cytoplasmic surface limit the rotation of the domain to the left.

Once these conditions were satisfied, small adjustments were made to allow the two domains to pack tightly together without substantial steric clashes with side chains in energetically favorable conformations, and to enhance energetically favorable interactions among polar atoms (criteria 4 and 5 of the Appendix). The docked structure was then minimized in vacuo before performing a 1-ns molecular dynamics simulation of the complex embedded in a POPE lipid bilayer, as described below. The two domains experienced substantial movements relative to each other in the first simulations that we performed, probably due to modeling errors. We used these results to reposition the domains to be nearer the conformation at the end of the simulation, and to remodel the L45 connecting segment in those simulations in which L45 did not remain stable. This process was repeated several times so that in our final simulations, very little movement occurred. The results of the simulations were used primarily to evaluate how the two domains may interact and to analyze the stability of the models rather than to predict the final structure within each domain, because the introduction of motion in molecular dynamics simulations necessitates some perturbation from the time-averaged crystal structure.

Similar rationale and methods were used to dock the two domains for transition and resting conformations. There are three reasons why the resting conformation is difficult to model: there are few experimental results with which to constrain the models, the presence of the rather long L45 linker on the cytoplasmic surface makes many positions plausible, and neither domain is modeled completely from a KvAP crystal structure. We favored models in which the location of the S1–S3a segments remain about the same as in the models of the open conformation because only small motions during activation have been observed for LRET (Cha and Bezanilla, 1997) and FRET (Larsson et al., 1996) probes attached to extracellular loops in *Shaker* channels. Although we have attempted to maximize interactions between intolerant residues, the hydrophobic nature of their exteriors makes it difficult to exclude the possibility of lipids separating the two domains, or just the inner halves of the domains in some conformations. In fact, after modeling the domains as described above, we noticed a hydrophobic cavity between the domains in the cytoplasmic half of the transmembrane region that we found difficult to eliminate by simply repositioning the voltage-sensing domain. In the open conformation this cavity could be filled by a phospholipid that has its headgroup on the cytoplasmic interface (see Fig. 6 and supplements to Fig. 8). We modeled the innermost resting conformation with three phospholipids between the domains (see Fig. 6 *H*). Negatively charged headgroups of these lipids interact with positively charged residues of S4 in the resting and most transition conformations. The presence of one or more lipids between the domains could reduce steric barriers to the movement of S4 during activation since lipid alkyl chains are substantially ''smoother'' and more flexible than are α-helices. Molecular dynamics simulations

with one to three lipids sandwiched between the domains produced lower root mean-square deviations (RMSDs) and lower energies for the closed conformations, but the results for the open conformation were not affected much. The conformation and position of the L45 segment is especially tenuous in our models of the resting conformation. We have assumed that it retains an α-helical conformation during gating, and have developed models in which it is either parallel to the surface of the membrane, as observed in the segments that precede the first transmembrane segment (analogous to S5) in Kir1.1 (Kuo et al., 2003) and KcsA (Cortes et al., 2001) channels, or extends into the cytoplasm if the movement of S4 is very large. In spite of the uncertainties, our ''best guess'' of how the domains dock illustrates the feasibility of the general mechanism, and provides a starting point for experimental testing of the models.

Molecular dynamics simulations

Recently, we have been performing molecular dynamics simulations of our membrane protein models embedded in a POPE lipid bilayer, with water on each side and within the pore of the channels, and K^+ ions in the selectivity filter. One-nanosecond simulations were performed as described in the Methods for a single voltage-sensing domain in the open (crystal structure 1) and four transition conformations embedded in the bilayer in the manner illustrated in Fig. 4 A. In similar simulations that we have performed using this methodology on crystal structures of KcsA (Doyle et al., 1998) and MscL (Chang et al., 1998; Rees et al., 1989) channels, we typically observed that the secondary structure remained intact and that the RMSD of the backbone from the starting conformation plateaus at 2–3 Å during the first 500 ps (unpublished results). The results for the voltage-sensing domain presented in Fig. 9 are thus typical, except that the RMSD of the open conformation is a bit lower than normal. This low RMSD supports our contention that Structure 2 has a stable native fold. The criterion of low RMSD to distinguish between models has been used previously in homology modeling studies (Arinaminpathy et al., 2003; Capener et al., 2000; Holyoake et al., 2003). The RMSDs calculated here for the transition and resting models are only slightly greater than those for Structure 2 (hypothetical open conformation), as would be expected for modeled structures that have small errors and/or that are transient configurations between more stable conformations. The root mean-square fluctuations shown in Fig. 9 indicate that the nonhelical regions are more dynamic, which is a typical result for simulations of proteins. Surprisingly, the energies calculated for the protein and its interactions with water and lipid are actually lower for the modeled transition conformations than are those of the crystal Structure 2. This lowering of the energy may have multiple causes: 1), several hydrophobic residues of S3b2 and the initial portion of S4 that are exposed
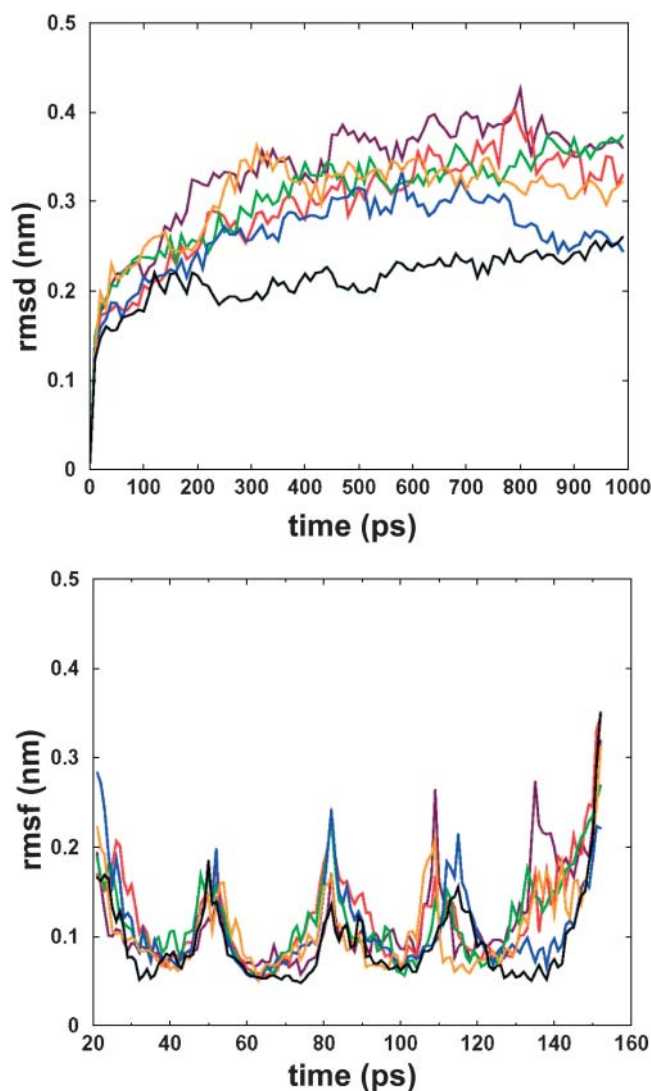

FIGURE 9 Results of molecular dynamics simulations of the voltage-sensing domain. (A) RMSD of the domain in the open Structure 2 (black), four intermediate (orange, yellow, green, cyan), and resting (blue) conformations. (B) Root mean-square fluctuations as a function of residue numbers of the same conformations. The residues corresponding to helices S1–L45 are denoted in the figure. The regions of higher fluctuations correspond to loops and termini. In the transition conformations the S4 segment is displaced one (orange), two (yellow), three (green), and four (cyan) helical screw steps inward from the open Structure 2 (black) conformation.

to the extracellular aqueous phase in the open conformation move to a more energetically favorable buried environment in the transition and resting conformations; 2), the number of salt bridges between positively charged S4 residues and negatively charged S1–S3 residues increases as S4 moves inward; and 3), the L45 helix moves to the surface of the bilayer where its hydrophobic face interacts with lipid alkyl chains while its hydrophilic face interacts with water and lipid headgroups.
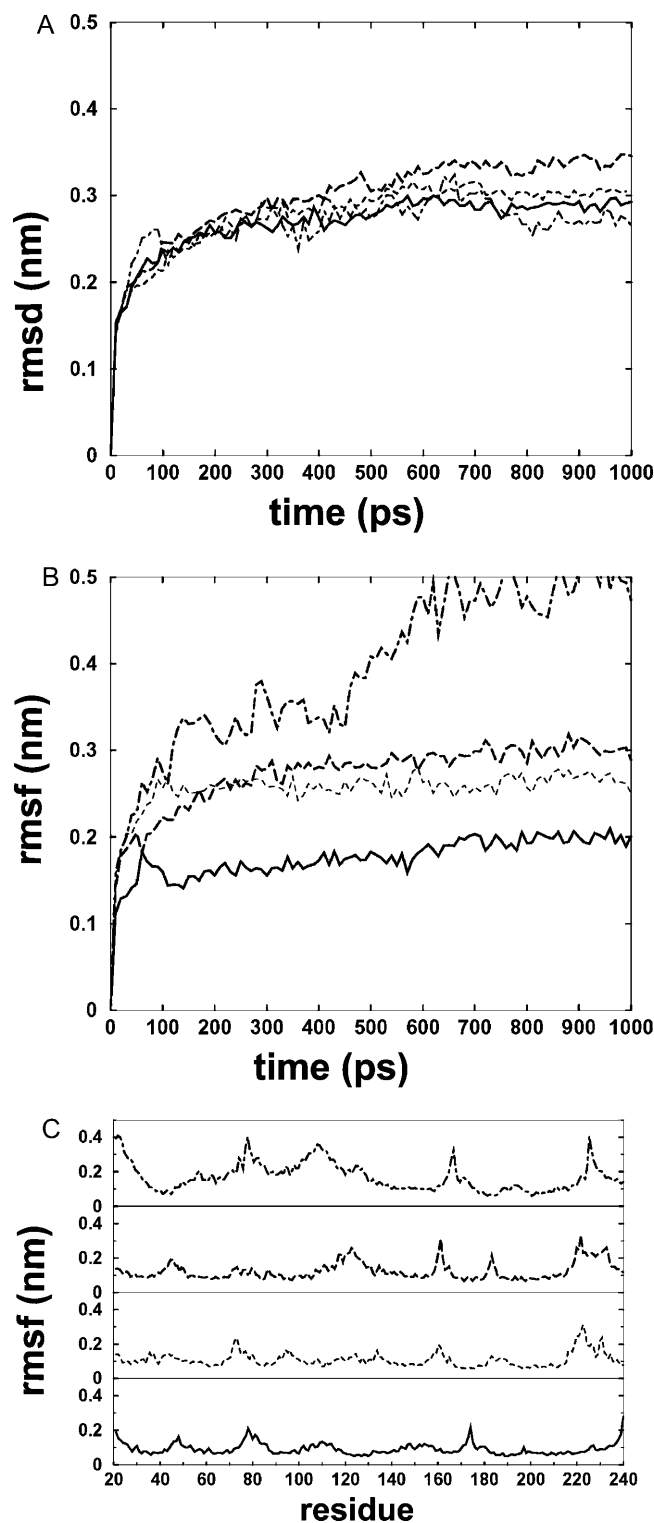
FIGURE 10 RMSDs from molecular dynamics simulations of our models of the open (*solid*), transition 4 (*long-dashed*), and resting (*thin-dashed*) conformations that include both domains and for Structure 1 for both the pore-forming (*dot-dashed*) (*A*) and voltage-sensing (*B*) domains. All four pore-forming domains were present in the simulations, but only one voltage-sensing domain was included. RMSD values were similar for the pore-forming domain in all four simulations. RMSD values for the voltage-sensing domain were exceptionally low for the open conformation, fairly

Molecular dynamics simulations of our final models that include both domains produce similar results: i.e., the structures are well maintained, the RMSD of the open voltage-sensing domain is exceptionally low, the RMSDs of the voltage-sensing domain in the modeled resting and transition conformation are comparable to those of the pore-forming domain, and the fluctuations are greater for the nonhelical regions (see Fig. 10). To save computational time, only one voltage-sensing domain was included along with all four pore-forming domains. This is justifiable because there are no direct interactions between adjacent voltage-sensing domains, i.e., the only protein-protein interactions are with the pore-forming domains, all of which were included and which remain relatively static. The voltage-sensing domain and lipid bilayer structures were substantially less stable during a molecular dynamics simulation of the full-length crystal Structure 1. The RMSD values continued to increase throughout the simulation and were quite high at the end of 1 ns (see Fig. 9). The planar lipid bilayer was disrupted during simulations of Structure 1, and water entered into the hydrophobic alkyl phase of the transmembrane region to hydrate the charged residues; i.e., the lipid-water system adapted to the structure of the protein. Furthermore, the polar ends and connecting loop of of S1 and S2 moved nearer the surfaces of the membrane. Since in Structure 1 the voltage sensor domains interact with each other, a simulation was done of the whole protein. Similar trends were observed in the RMSDs vis-à-vis the voltage sensor domain, i.e., the RMSD of the voltage sensor domain was very high at the end of 1 ns (see supplementary figure).

DISCUSSION AND CONCLUSIONS

Here we have demonstrated that a rather conventional helical screw model that has a traditional transmembrane topology can be developed from the two KvAP crystal structures in a manner consistent with experimental results and theoretical constraints. We used portions of the KvAP crystal structures that are likely to have native folds; i.e., the pore-forming domain from Structure 1 and the voltage-sensing domain from Structure 2. In developing models of membrane proteins we evaluate their energetic, evolutionary, and experimental soundness. The experimental soundness of our models relative to alternative models is discussed in the accompanying article because most of the experimental studies have been performed on the *Shaker* channel.

typical (about the same as for the pore-forming domain) for the resting and transition 4 conformations, and very high for Structure 1. (*C*) Root mean-square fluctuations (rmsf) as a function of residue numbers for the same conformations. The line styles are same as in *A*. The regions of higher fluctuations correspond to loops and termini.

There are several indications that all conformations of our models are energetically sound: 1), the RMSDs of the structures are low during the molecular dynamics simulations; 2), almost all polar atoms (especially the positively charged S4 atoms) can form hydrogen bonds or salt bridges with polar atoms of the protein, water, or lipid headgroups in all conformations; 3), few hydrophobic residues are fully exposed to water; and 4) almost all residues and side chains have energetically favorable conformations (see Table 1 of supplementary material). In contrast, the paddle model postulates that the charged residues of S4 move through the hydrophobic lipid phase of the membrane during activation. Although it is difficult to quantitatively compare the energies of these models, the electrostatics of our models are clearly superior in lowering the energy of moving S4 charges through the membrane's electric field and in increasing the probability that the side chains will remain protonated throughout the movement. It has been asserted that S4 is not exposed to lipid in conventional models (Jiang et al., 2003b); however, in our models much of S4 is exposed to lipid alkyl chains of both the bulk phase as well as lipids introduced in between the two domains. This lipid exposure is always energetically favorable in our models because hydrophobic interactions involve only residues with apolar side chains and lipid interactions with positively charged S4 side chains involve polar lipid headgroups. This type of lipid exposure may be important in reducing energy barriers to movement of S4, and helps explain why attachment of large hydrophobic moieties, such as biotin molecules, to S4 does not prevent its movement (Jiang et al., 2003b).

Our models are evolutionarily sound as well:

1. Almost all residue profile positions that are poorly conserved in alignments of closely related channels are on the surface and have compositions consistent with their exposure to lipid alkyl chains, lipid headgroups, or water.
2. Functionally important sites are highly conserved in alignments of distantly related families that possess the same function (e.g., the core of the voltage-sensing domain of transition conformations (see Fig. 5)).

We are currently developing similar models of numerous homologous channels, which will be published elsewhere. Our preliminary results indicate that the basic mechanism proposed here can work for all voltage-gated channels (see criterion 13 of the Appendix), but the magnitude of the movement of S4 and the way that the two domains interact may differ from channel to channel.

All models of voltage gating still have many uncertainties and ambiguities. Questions raised by our models, and ways to experimentally test many of our hypotheses, are discussed in the supplement of the accompanying article. The merits of our models are compared to those of other models in the accompanying article. We hope our models will contribute to the multidisciplinary approaches to determine the actual structure and gating mechanisms of these channels.

APPENDIX

Modeling criteria

The assumptions, criteria, and principles that we use in developing models of membrane proteins are described below. Most of these criteria have been used previously by us and other groups; however, we have recently incorporated results of molecular dynamics simulations in evaluating our models. Our criteria can be classified into three categories: energetic, evolutionary, and experimental.

Energetic criteria

1. Physical properties of the lipid hydrocarbon phase of the transmembrane region resemble those of a hydrophobic organic solvent slab that is ~25 Å thick (White and Wimley, 1998).
2. Almost all hydrogen bond donor and acceptor atoms should form hydrogen bonds with other protein groups, water, or lipid headgroups. This requires most side chains that are exposed to lipid alkyl chains to be hydrophobic, segments in contact with the lipid alkyl chains to have a regular secondary structure in which most polar backbone atoms bind to other polar backbone atoms, and polar termini of α-helices not to be exposed to lipid alkyl chains.
3. Side chains that can be positively or negatively charged (arginine, lysine, histidine, glutamate, and aspartate) will rarely be exposed exclusively to alkyl chains in the core of the transmembane hydrophobic slab. If they are exposed in the lipid core, then they will not be charged. (These criteria are based on calculations that the energy to transfer any of the charged side chains from water to an organic solvent such as hexane is substantially larger than the energy to neutralize the group at neutral pH (calculated by the equation $E = \pm 2.3RT(\text{pK} - \text{pH})$) and then to transfer the uncharged side chain from water to hexane (Lazaridis, 2003).)
4. Most interactions among side chains or between side chains and backbone atoms should be energetically favorable, especially if the residues are buried within the protein. Energetically favorable side-chain interactions are disulfide bridges, salt bridges, hydrogen bonds, aromatic-aromatic interactions, aromatic-positive charged interactions, and hydrophobic interactions. (In the models presented here, most charged groups of the S1–S4 bundle form salt bridges.) Interactions of positively and negatively charged side chains with α-helix C- and N-termini, respectively, are also energetically favorable. (Our KvAP models have several such interactions.)
5. Most backbone and side-chain conformations should be energetically favorable and occur frequently in proteins of known conformation (Ponder and Richards, 1987).
6. Most transmembrane segments will be α-helices unless the protein forms a transmembrane β barrel. Positions where the structure is not helical or where α-helices are broken or distorted will tend to contain indels in multisequence alignments and/or residues with low helical propensity; especially proline, but also glycine, serine, threonine, asparagines, and aspartate. (The secondary structure of models developed using these criteria (Durell et al., 1998) correspond closely to that of the KvAP crystal structures. In the models presented here, these criteria are used to propose a hinge region in the S3b helix of KvAP.)
7. In packing transmembrane α-helices, a preference should be given to arrangements in which adjacent helices can pack according to "knobs-into-holes" and/or "ridges-into-grooves" packing theory (Bowie, 1997). (This criterion is weak, reflecting some statistical preference, and exceptions are often observed in membrane proteins. Most of the interactions between helices in the pore-forming domain of the K^+ channel crystal structures and in Structure 2 of the voltage-sensing domain have crossing consistent with either 3-4 (from 0 to $-40°$) or 4-4 (20–60°) ridges-into-grooves packing. This criterion does not affect the

models presented here because most helix-helix interactions are dictated by the crystal structures.)

8. Most transmembrane helices should pack tightly next to other helices (Eilers et al., 2002). (The helices of the voltage-sensing domain are packed more tightly in Structure 2 and in our models of transition and resting conformations than they are in Structure 1.)

9. The protein should form a solid barrier between the lipid alkyl chains and the water- and ion-filled pore in all conformations. (This criterion is satisfied for the pore-forming domain of all of the K^+ channel crystal structures; but lipid headgroups may line part of the inner crevasse.)

10. The correct model of a relatively stable conformation should deviate little during an unrestrained molecular dynamics simulation of the protein embedded in a lipid bilayer with water on each side of the membrane and in the pore. (The RMSD of the voltage-sensor S1–S4 region of Structure 2 and our models of KvAP during a 1 ns molecular dynamics simulation is much lower than that of the S1–S4 portion of Structure 1.)

Evolutionary criteria

11. Residues that are on the surface of the protein in all conformations will tend to be poorly conserved among closely related proteins unless they are at an active site or affect the secondary structure; e.g., a conserved proline that breaks or distorts an α-helix can be on the surface. If the residue is exposed to lipid alkyl chains, most side chains will be hydrophobic (V, L, I, M, F) or ambivalent (A, G, T, S, P). If it is in the transition region between the alkyl and headgroup lipid regions, the position will also tolerate aromatics (Y and W) and positively charged (K, R, H) or noncharged polar (Q and N) residues. If it is exposed to the aqueous phase, most residues will be hydrophilic (D, E, Q, N, K, R), ambivalent (G, C, S, T, H), or have a high propensity for coiled structures and turns (P, G, S, T, N, D). Most insertions and deletions (indels) will occur in aqueous exposed loops. Experimentally introduced substitutions at these tolerant surface positions will not dramatically alter the properties of the protein as long as the general polarity of the side chain is not altered dramatically. These criteria can be used to position lipid-exposed α-helices by orienting poorly conserved hydrophobic faces toward the lipid alkyl region and positioning the helix so that predicted transitions from alkyl-exposed to headgroup-exposed residues occur on each side of the postulated hydrophobic slab of the membrane.

12. Most residues that are highly conserved among closely related proteins will be in the core of the protein and/or involved in functionally important mechanisms. Residues that are highly conserved among distantly related protein families will tend to form clusters at functionally important sites as long as the function is conserved among the families. (In the models presented here, the core of Structure 2 is highly conserved among closely related channels and a cluster of residues in the core of the voltage-sensing domain of some transition conformations is highly conserved among numerous distantly related families of voltage-gated channels. The selectivity filter is well conserved among K^+ channels but is poorly conserved between K^+ and channels that are selective for other ions.)

13. Portions of homologous proteins that can be aligned unambiguously have similar backbone structures. It should be possible to model the backbone structure of such regions of all homologs on at least some conformations of the model of the initial protein. (Homologous sequences with shorter loop regions can constrain the locations of transmembrane segments; e.g., we have demonstrated that proteins with much shorter S3-S4 linkers and shorter L45 segments can be modeled using the backbone structure of some of the KvAP models of transition conformations.)

Experimental criterion

14. The correct model should be consistent with and explain most experimental results. (This criterion will be discussed extensively in the accompanying on *Shaker* channel models.)

The controversy about the structure of KvAP and its gating mechanism involves more than the structure and gating mechanisms of voltage-gated channels. It also involves how confident we can be about the correctness of crystal structures of membrane proteins, how much we can trust results of mutagenesis experiments to provide easily interpretable information about the structure and functional mechanisms of membrane proteins, and the validity of criteria that we and others use in developing models of membrane proteins. If the paddle model is correct, then results of many mutagenesis experiments have been uninformative and/or misinterpreted, and our modeling criteria are invalid for this type of membrane protein. However, if our models are approximately correct, and crystal Structure 1 and the paddle model derived from it are nonnative and incorrect, then the role of mutagenesis and molecular modeling in analyzing the correctness of protein structures and in developing models of the structure and functional mechanisms of membrane proteins would be validated. Many of our criteria are not absolute, but rather reflect perceived statistical tendencies that, unfortunately, have not been rigorously quantified. Thus, exceptions are possible and uncertainties exist. The standard way to validate and quantify the kind of evolutionary criteria that we use is to perform statistical analyses of known protein structures. This approach is complicated for membrane proteins because the database of known structures is relatively small, and we do not know whether or not all of them have a native conformation. Also, evaluation of some of our criteria require knowing all functionally important conformations of the protein; e.g., in our MscL models (Sukharev et al., 2001a,b), some highly conserved residues are exposed on the surface of the protein in the crystal structures, but become buried and/or interact with other highly conserved residues in other conformations. Unfortunately, for most membrane proteins that have been crystallized, only one conformation has been determined. Evaluation of some of our criteria also requires knowing whether other proteins or subunits interact with the modeled protein; and if so, where this interaction occurs. We acknowledge that some of our modeling criteria will be invalid if the protein perturbs the planar lipid bilayer structure substantially, and that such perturbation is likely for some other types of membrane channels. In fact, we have proposed models of channels formed by helical peptides in which the lipid is perturbed during formation of the pores, and is sometimes incorporated into the structure of the pore (Raghunathan et al., 1990; Durell et al., 1992; Cruciani et al., 1992). We also suspect that substantial lipid perturbation occurs when large polar moieties of the colicin 1a channel protein cross the membrane (Slatin et al., 1994) to form ion channels. Thus, criteria that are valid for relatively static proteins that do not perturb the lipid bilayer may not be appropriate for more dynamic proteins.

SUPPLEMENTARY MATERIAL

An online supplement to this article can be found by visiting BJ Online at http://www.biophysj.org.

REFERENCES

Aggarwal, S. K., and R. MacKinnon. 1996. Contribution of the S4 segment to gating charge in the *Shaker* K+ channel. *Neuron.* 16:1169–1177.

Altschul, S. F., T. L. Madden, A. A. Schaffer, J. Zhang, Z. Zhang, W. Miller, and D. J. Lipman. 1997. Gapped BLAST and PSI-BLAST: a new generation of protein database search programs. *Nucleic Acids Res.* 25:3389–3402.

Arinaminpathy, Y., P. C. Biggin, I. H. Shrivastava, and M. S. Sansom. 2003. A prokaryotic glutamate receptor: homology modelling and molecular dynamics simulations of GluR0. *FEBS Lett.* 553:321–327.

Baldwin, J. M., G. F. Schertler, and V. M. Unger. 1997. An alpha-carbon template for the transmembrane helices in the rhodopsin family of G-protein-coupled receptors. *J. Mol. Biol.* 272:144–164.

Berger, O., O. Edholm, and F. Jahnig. 1997. Molecular dynamics simulations of a fluid bilayer of dipalmitoylphosphatidylcholine at full hydration, constant pressure, and constant temperature. *Biophys. J.* 72:2002–2013.

Bezanilla, F. 2002. Voltage sensor movements. *J. Gen. Physiol.* 120:465–473.

Bowie, J. U. 1997. Helix packing in membrane proteins. *J. Mol. Biol.* 272:780–789.

Brooks, B. R., R. E. Bruccoleri, B. D. Olafson, D. J. States, S. Swaminathan, and M. Karplus. 1983. CHARMM: a program for macromolecular energy minimization and dynamic calculations. *J. Comput. Chem.* 4:187–217.

Capener, C. E., I. H. Shrivastava, K. M. Ranatunga, L. R. Forrest, G. R. Smith, and M. S. Sansom. 2000. Homology modeling and molecular dynamics simulation studies of an inward rectifier potassium channel. *Biophys. J.* 78:2929–2942.

Cha, A., and F. Bezanilla. 1997. Characterizing voltage-dependent conformational changes in the *Shaker* K+ channel with fluorescence. *Neuron.* 19:1127–1140.

Chang, G., R. H. Spencer, A. T. Lee, M. T. Barclay, and D. C. Rees. 1998. Structure of the MscL homolog from Mycobacterium tuberculosis: a gated mechanosensitive ion channel. *Science.* 282:2220–2226.

Cohen, B. E., M. Grabe, and L. Y. Jan. 2003. Answers and questions from the KvAP structures. *Neuron.* 39:395–400.

Cortes, D. M., L. G. Cuello, and E. Perozo. 2001. Molecular architecture of full-length KcsA: role of cytoplasmic domains in ion permeation and activation gating. *J. Gen. Physiol.* 117:165–180.

Cruciani, R. A., J. L. Barker, S. R. Durell, G. Raghunathan, H. R. Guy, M. Zasloff, and E. F. Stanley. 1992. Magainin 2, a natural antibiotic from frog skin, forms ion channels in lipid bilayer membranes. *Eur. J. Pharmacol.* 226:287–296.

Doyle, D. A., C. J. Morais, R. A. Pfuetzner, A. Kuo, J. M. Gulbis, S. L. Cohen, B. T. Chait, and R. MacKinnon. 1998. The structure of the potassium channel: molecular basis of K+ conduction and selectivity. *Science.* 280:69–77.

Durell, S. R., and H. R. Guy. 1999. Structural models of the KtrB, TrkH, and Trk1,2 symporters based on the structure of the KcsA K(+) channel. *Biophys. J.* 77:789–807.

Durell, S. R., and H. R. Guy. 2001. A family of putative Kir potassium channels in prokaryotes. *BMC Evol Biol.* 1:14.

Durell, S. R., Y. Hao, and H. R. Guy. 1998. Structural models of the transmembrane region of voltage-gated and other K+ channels in open, closed, and inactivated conformations. *J. Struct. Biol.* 121:263–284.

Durell, S. R., G. Raghunathan, and H. R. Guy. 1992. Modeling the ion channel structure of cecropin. *Biophys. J.* 63:1623–1631.

Eilers, M., A. B. Patel, W. Liu, and S. O. Smith. 2002. Comparison of helix interactions in membrane and soluble alpha-bundle proteins. *Biophys. J.* 82:2720–2736.

Elinder, F., P. Arhem, and H. P. Larsson. 2001a. Localization of the extracellular end of the voltage sensor S4 in a potassium channel. *Biophys. J.* 80:1802–1809.

Elinder, F., R. Mannikko, and H. P. Larsson. 2001b. S4 charges move close to residues in the pore domain during activation in a K channel. *J. Gen. Physiol.* 118:1–10.

Gandhi, C. S., E. Clark, E. Loots, A. Pralle, and E. Y. Isacoff. 2003. The orientation and molecular movement of a k(+) channel voltage-sensing domain. *Neuron.* 40:515–525.

Gandhi, C. S., and E. Y. Isacoff. 2002. Molecular models of voltage sensing. *J. Gen. Physiol.* 120:455–463.

Guy, H. R. 1990. Models of voltage- and transmitter-activated channels based on their amino acid sequences. *In* Monovalent Cations in Biological Systems. C. A. Pasternak, editor. CRC Press, Boca Raton, FL. 31–38.

Guy, H. R., and S. R. Durell. 1994. Using sequence homology to analyze the structure and function of voltage-gated ion channel proteins. *Soc. Gen. Physiol. Ser.* 49:197–212.

Guy, H. R., and P. Seetharamulu. 1986. Molecular model of the action potential sodium channel. *Proc. Natl. Acad. Sci. USA.* 83:508–512.

Henikoff, S., and J. G. Henikoff. 1994. Position-based sequence weights. *J. Mol. Biol.* 243:574–578.

Holyoake, J., C. Domene, J. N. Bright, and M. S. Sansom. 2003. KcsA closed and open: modelling and simulation studies. *Eur Biophys J.*

Hong, K. H., and C. Miller. 2000. The lipid-protein interface of a *Shaker* K(+) channel. *J. Gen. Physiol.* 115:51–58.

Jiang, Y., A. Lee, J. Chen, M. Cadene, B. T. Chait, and R. MacKinnon. 2002. Crystal structure and mechanism of a calcium-gated potassium channel. *Nature.* 417:515–522.

Jiang, Y., A. Lee, J. Chen, V. Ruta, M. Cadene, B. T. Chait, and R. MacKinnon. 2003a. X-ray structure of a voltage-dependent K+ channel. *Nature.* 423:33–41.

Jiang, Y., V. Ruta, J. Chen, A. Lee, and R. MacKinnon. 2003b. The principle of gating charge movement in a voltage-dependent K+ channel. *Nature.* 423:42–48.

Kumanovics, A., G. Levin, and P. Blount. 2002. Family ties of gated pores: evolution of the sensor module. *FASEB J.* 16:1623–1629.

Kuo, A., J. M. Gulbis, J. F. Antcliff, T. Rahman, E. D. Lowe, J. Zimmer, J. Cuthbertson, F. M. Ashcroft, T. Ezaki, and D. A. Doyle. 2003. Crystal structure of the potassium channel KirBac1.1 in the closed state. *Science.* 300:1922–1926.

Laine, M., M. C. Lin, J. P. Bannister, W. R. Silverman, A. F. Mock, B. Roux, and D. M. Papazian. 2003. Atomic proximity between S4 segment and pore domain in *Shaker* potassium channels. *Neuron.* 39:467–481.

Larsson, H. P., O. S. Baker, D. S. Dhillon, and E. Y. Isacoff. 1996. Transmembrane movement of the *Shaker* K+ channel S4. *Neuron.* 16:387–397.

Laskowski, R., M. McArthur, D. Moss, and J. Thornton. 1993. PROCHECK: A program to check for stereochemical quality of protein structures. *J. Appl. Crystallogr.* 26:283–291.

Lazaridis, T. 2003. Effective energy function for proteins in lipid membranes. *Proteins.* 52:176–192.

Li-Smerin, Y., D. H. Hackos, and K. J. Swartz. 2000a. A localized interaction surface for voltage-sensing domains on the pore domain of a K+ channel. *Neuron.* 25:411–423.

Li-Smerin, Y., D. H. Hackos, and K. J. Swartz. 2000b. alpha-helical structural elements within the voltage-sensing domains of a K(+) channel. *J. Gen. Physiol.* 115:33–50.

Lu, Z., A. M. Klem, and Y. Ramu. 2001. Ion conduction pore is conserved among potassium channels. *Nature.* 413:809–813.

Miller, G. 2003. Neuroscience. The puzzling portrait of a pore. *Science.* 300:2020–2022.

Monks, S. A., D. J. Needleman, and C. Miller. 1999. Helical structure and packing orientation of the S2 segment in the *Shaker* K+ channel. *J. Gen. Physiol.* 113:415–423.

Ng, P. C., J. G. Henikoff, and S. Henikoff. 2000. PHAT: a transmembrane-specific substitution matrix. Predicted hydrophobic and transmembrane. *Bioinformatics.* 16:760–766.

Patton, D. E., J. W. West, W. A. Catterall, and A. L. Goldin. 1993. A peptide segment critical for sodium channel inactivation functions as an inactivation gate in a potassium channel. *Neuron.* 11:967–974.

Ponder, J. W., and F. M. Richards. 1987. Tertiary templates for proteins. Use of packing criteria in the enumeration of allowed sequences for different structural classes. *J. Mol. Biol.* 193:775–791.

Raghunathan, G., P. Seetharamulu, B. R. Brooks, and H. R. Guy. 1990. Models of delta-hemolysin membrane channels and crystal structures. *Proteins.* 8:213–225.

Rees, D. C., L. DeAntonio, and D. Eisenberg. 1989. Hydrophobic organization of membrane proteins. *Science.* 245:510–513.

Ruta, V., Y. Jiang, A. Lee, J. Chen, and R. MacKinnon. 2003. Functional analysis of an archaebacterial voltage-dependent K+ channel. *Nature.* 422:180–185.

Santacruz-Toloza, L., Y. Huang, S. A. John, and D. M. Papazian. 1994. Glycosylation of *Shaker* potassium channel protein in insect cell culture and in Xenopus oocytes. *Biochemistry.* 33:5607–5613.

Schoppa, N. E., K. McCormack, M. A. Tanouye, and F. J. Sigworth. 1992. The size of gating charge in wild-type and mutant *Shaker* potassium channels. *Science.* 255:1712–1715.

Slatin, S. L., X. Q. Qiu, K. S. Jakes, and A. Finkelstein. 1994. Identification of a translocated protein segment in a voltage-dependent channel. *Nature.* 371:158–161.

Starace, D. M., and F. Bezanilla. 2004. A proton pore in a potassium channel voltage sensor reveals a focused electric field. *Nature.* 427:548–553.

Sukharev, S., M. Betanzos, C. S. Chiang, and H. R. Guy. 2001a. The gating mechanism of the large mechanosensitive channel MscL. *Nature.* 409:720–724.

Sukharev, S., S. R. Durell, and H. R. Guy. 2001b. Structural models of the MscL gating mechanism. *Biophys. J.* 81:917–936.

Swanson, E. 1995. PSSHOW version 1.9. University of Washington, Seattle, WA.

Thompson, J. D., D. G. Higgins, and T. J. Gibson. 1994. CLUSTAL W: improving the sensitivity of progressive multiple sequence alignment through sequence weighting, position-specific gap penalties and weight matrix choice. *Nucleic Acids Res.* 22:4673–4680.

Tiwari-Woodruff, S. K., M. A. Lin, C. T. Schulteis, and D. M. Papazian. 2000. Voltage-dependent structural interactions in the *Shaker* K(+) channel. *J. Gen. Physiol.* 115:123–138.

White, S. H., and W. C. Wimley. 1998. Hydrophobic interactions of peptides with membrane interfaces. *Biochim. Biophys. Acta.* 1376:339–352.

Yang, N., A. L. George, Jr., and R. Horn. 1996. Molecular basis of charge movement in voltage-gated sodium channels. *Neuron.* 16:113–122.

Zhou, Y., J. H. Morais-Cabral, A. Kaufman, and R. MacKinnon. 2001. Chemistry of ion coordination and hydration revealed by a K+ channel-Fab complex at 2.0 Åresolution. *Nature.* 414:43–48.